We are IntechOpen, the world's leading publisher of Open Access books Built by scientists, for scientists

6,900
Open access books available

185,000
International authors and editors

200M
Downloads

154
Countries delivered to

Our authors are among the

TOP 1%
most cited scientists

12.2%
Contributors from top 500 universities

CLARIVATE ANALYTICS

BOOK CITATION INDEX

INDEXED

WEB OF SCIENCE™

Selection of our books indexed in the Book Citation Index
in Web of Science™ Core Collection (BKCI)

Interested in publishing with us?
Contact book.department@intechopen.com

Vibration of Satellite Solar Array Paddle Caused by Thermal Shock When a Satellite Goes Through the Eclipse

Mitsushige Oda, Akihiko Honda, Satoshi Suzuki and
Yusuke Hagiwara

Additional information is available at the end of the chapter

1. Introduction

Remote sensing satellites take images of the earth's surface in observing various activities by humans or nature. In order to obtain precise and high-resolution images from a satellite in Low Earth Orbit (LEO) at an attitude of 500 to 900 kilometers, the satellite's attitude must be stable when the onboard camera sensors take images of surface activities on the earth. Should the attitude stability of the satellite be disturbed while such images are being taken, poor image quality would probably result.

The fact that images taken when a satellite goes into or out from an eclipse do not provide good accuracy—due to degraded altitude stability at such timings—has been known for years. Such phenomena has long been attributed to the deformation and vibration of the satellite's solar array paddle that occurs when the satellite go into or out from an eclipse, along with the instantaneous change in solar energy received by the satellite. Several trials were conducted in the past to identify the phenomena, but all failed to achieve reasonable results.

2. Measurement of solar array paddle motion

The reason why past trials failed to observe the phenomena described above might be that the motion of the solar array paddle is too small or slow to be observed by such onboard sensors as an accelerometer. Therefore, JAXA decided to measure the phenomena by using an onboard camera that was originally mounted on the satellite to monitor solar array pad-

dle deployment (Fig. 2). (For GOSAT, the solar array paddle consists of three solar panels, a yoke, wires that control deploying speed, and hinge/latch mechanisms that connect the panels and yoke.) A small CCD/CMOS camera (Fig. 4) is mounted on most JAXA satellites to monitor solar array paddle deployment, as failure to deploy the solar array paddle would become critical failure of the satellite itself. We thus developed a system that uses this CMOS camera to measure the distortion and vibration of the solar array paddle, with said vibration being measured as follows:

1. Attach small reflective target markers at the end of the paddle (as shown in Fig. 3).

2. Take images from this camera and transmit them to the on-ground station. Fig. 2 is an image taken by the camera.

3. Identify the locations of the target markers in the camera view with image processing.

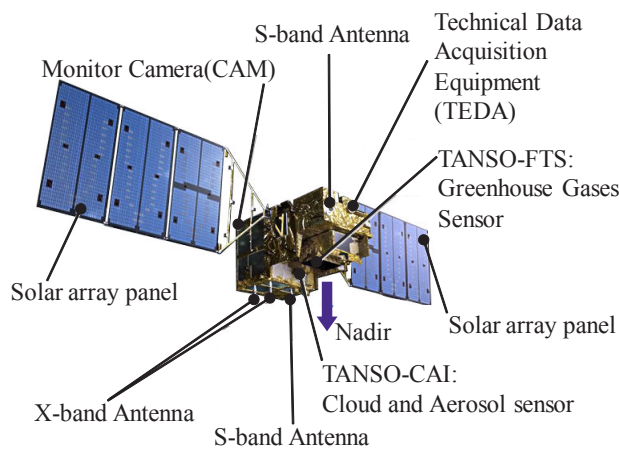4. Calculate displacement from the predicted target marker locations.

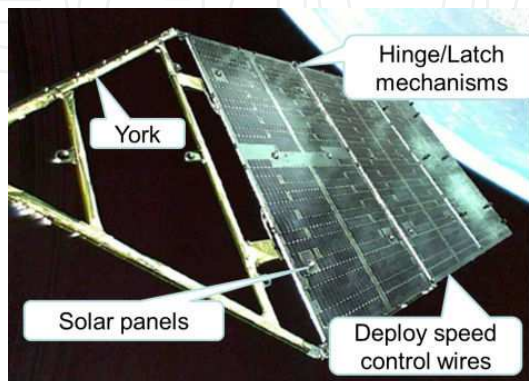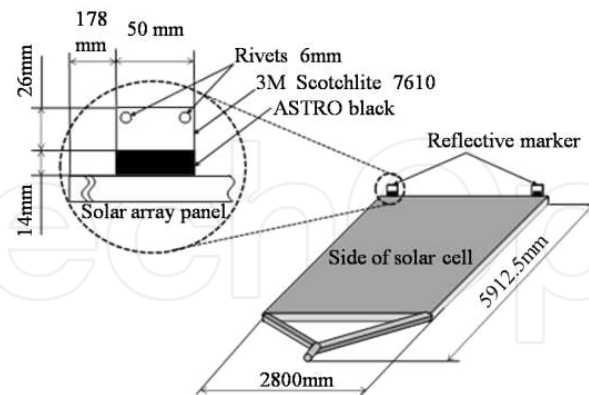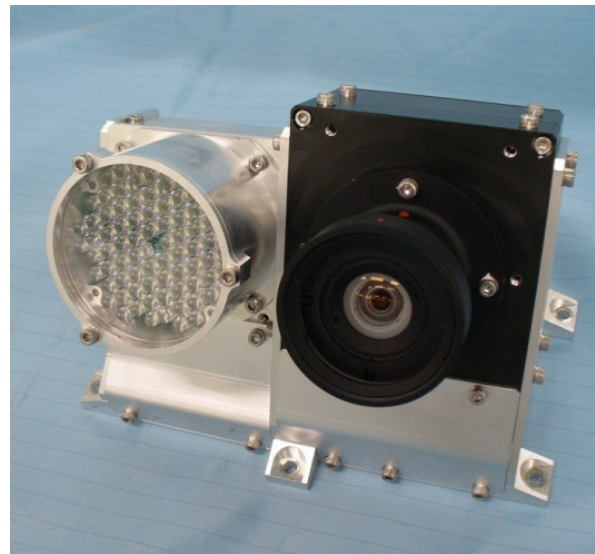**Figure 1.** JAXA's earth observation satellite "GOSAT"

Figure 2. Image taken by camera

For GOSAT, the solar array paddle consists of three solar panels, a yoke, wires that control deploying speed, and hinge/latch mechanisms that connect the panels and yoke.


Figure 3. Target markers on the solar array paddle

Figure 4. CMOS camera and LED lights

3. Measurement algorithm

As the onboard camera used for this experiment was originally designed to monitor the deployment of a folded solar array paddle, its field of view is thus as wide as 90 [deg] (Fig. 5), while the camera's number of pixels is limited to SXGA (1280 X 1024 pixels). The size of the markers is also limited to 50 [mm] X 26 [mm], while distance from the camera to the target markers is as far as 6 [m]. These constraints mean that one pixel of the camera is equivalent to 7 [mm] at the target marker's position. Therefore, a technique for processing sub-pixel level image data is required to identify deformation of the solar array paddle.
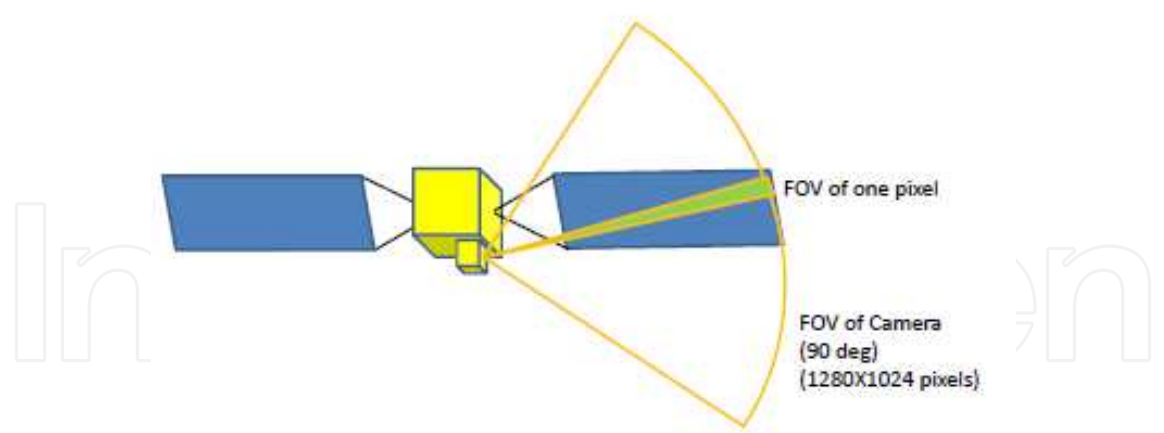
Figure 5. Constraints on image data processing

4. Previous results

The initial results of these measurements were reported in another paper in this series (Oda et al., 2011). Fig. 6 shows typical results. It shows an offset of a few millimeters appeared when solar array paddle illuminated by the Sun and when in an eclipse. However, these results pose certain difficulties in explaining the phenomena, as the tendency of the solar array paddle to bend does not agree with the observation results and conventional research.
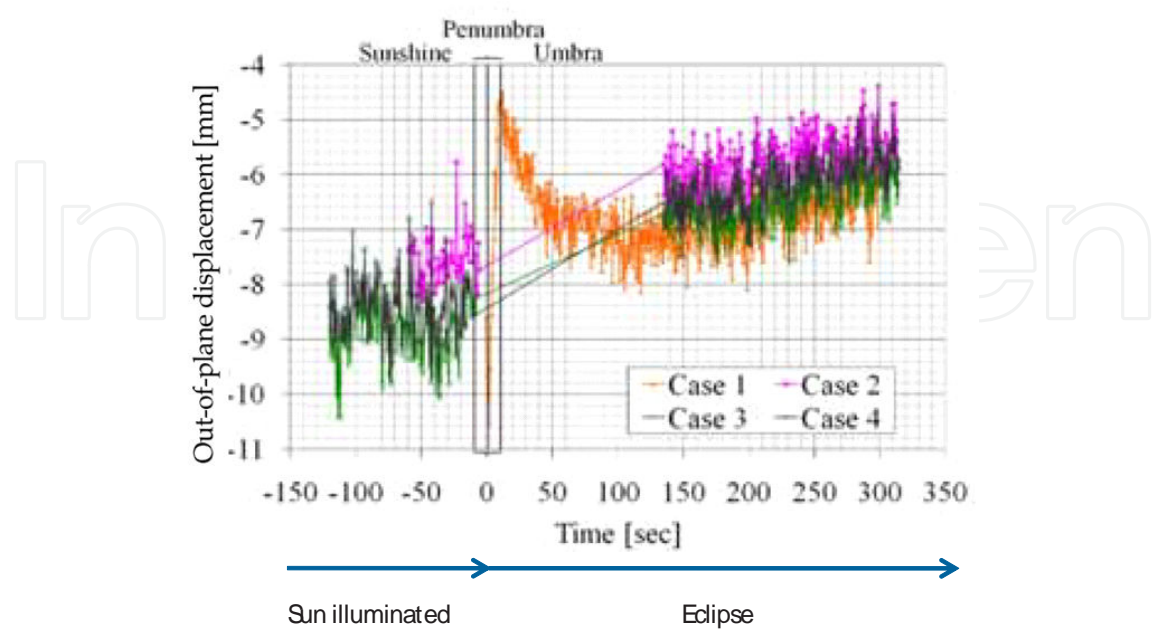

Figure 6. Motion of the solar array paddle's tip position as estimated from onboard camera images

Since solar energy from the Sun is the primary energy provided on the satellite and its solar array paddle, deformation of the solar array paddle should occur so that its structure on the Sun side is extended and causes bending of the solar panels toward the rear side of the solar array paddle. Previous results have indicated that the solar array paddle will bend toward its solar cell side, however. When the initial results of these measurements were recorded, we were unable to identify the source of the errors.

5. Revised results

Fig. 6 shows a sudden offset in the motion of the solar array paddle. When the solar array paddle is straight, the value of displacement may indicate -12 or -11 [mm] in Fig.6. Although we attempted to identify cause of this offset, we could not imagine a proper mechanism that would produce such a direction. We therefore assumed that the previous image data processing contained unidentified data processing errors, and consequently modified the algorithm that identifies the target markers. The earlier version of the algorithm used to identify locations of the target markers assumed such highly illuminated areas as those of the target markers. This algorithm works well when the markers are brightly illuminated. When the target markers are weakly illuminated, however, we found that this algorithm produces some data processing errors.

Fig. 7 and Fig. 8 illustrate the difference described above. Fig. 7 is based on the previous algorithm. The areas enclosed by a yellow line are pixels that are brighter than the threshold level and thus can be assumed to be the target markers as based on sub-pixel level image data processing. The red cross indicates the center position of the marker.
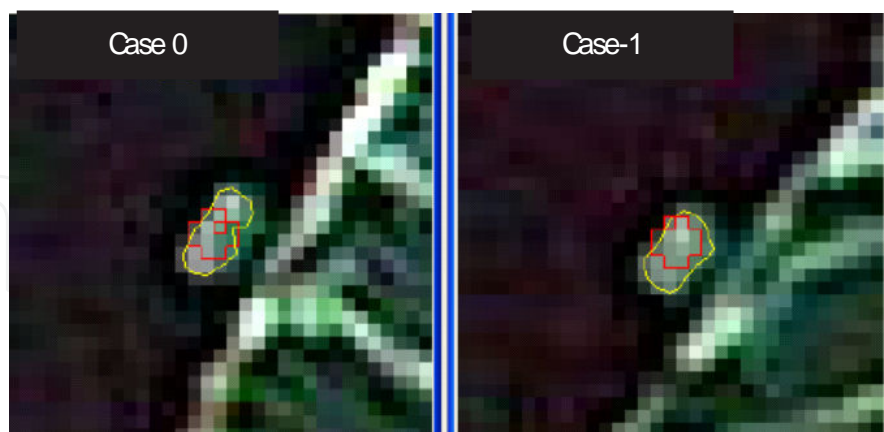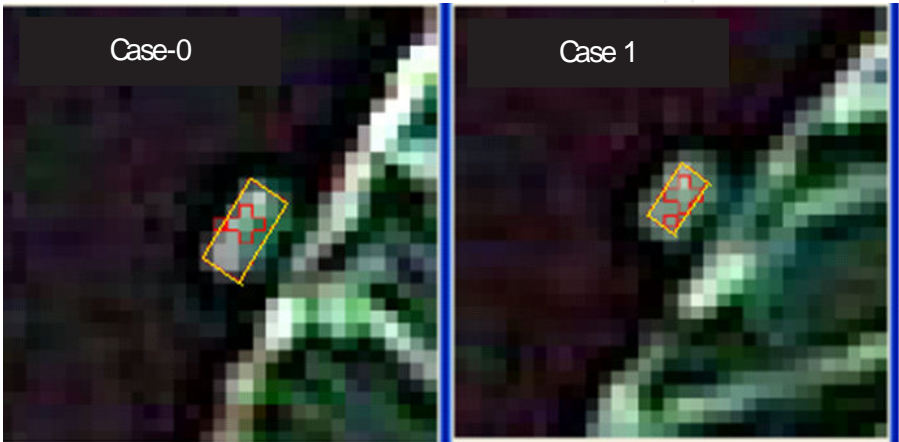

Figure 7. Target markers estimated by the previous algorithm under weak illumination. The areas of target markers assumed by the previous algorithm are smaller than the actual target marker size.

Fig. 7 shows that the sizes of the estimated target markers are smaller than the actual target markers. We therefore modified the algorithm used to estimate the area of a target marker so that the size of the predicted target marker is similar to that calculated from the actual

target marker. This modification worked well to identify the target marker and its displacement. Fig. 8 is a result based on the revised algorithm. In this revised algorithm, the areas to be considered target makers are decided based on the brightness level of each pixel and also on the size of the areas considered to be target markers. When an assumed target marker is too small, then the threshold level of brightness is automatically adjusted to meet the possible size of the target markers.

Finally, Fig. 9 shows the motion of a target marker as based on the revised algorithm. We can see that the estimated motion of the solar array paddle has less dispersion.

Figure 8. Target markers estimated by the revised algorithm
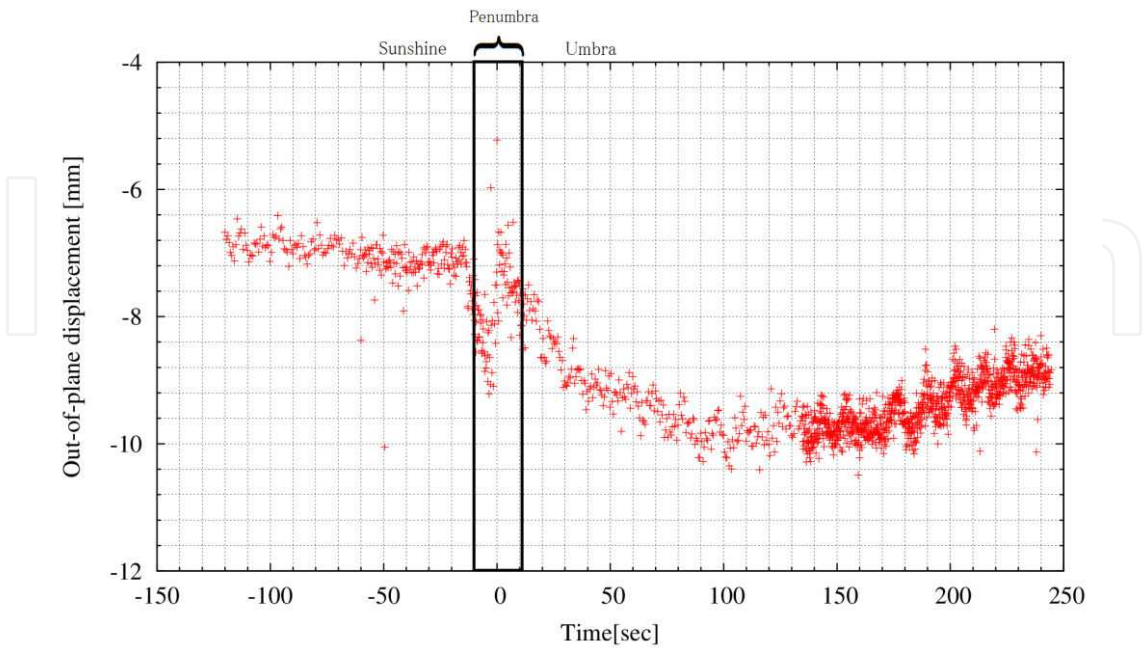
Figure 9. Displacement of GOSAT's solar array paddle when going into eclipse

From these data, we can conclude that the temperature of the solar array paddle changes steadily but not drastically, depending on its thermal capacity. And we also assume like as following.

1. When the solar array paddle is illuminated by the Sun, its temperature is governed by solar energy from the Sun (as well as that reflected from Earth).

2. When in an eclipse, the solar array paddle shows lower temperature depending on its thermal capacity. When the satellite's LST (Local Sun Time) is around noon, the solar cell side of the panels faces the Earth and receives solar radiation from Earth. In the evening and the early morning of satellite LST, however, both sides of the solar panels face toward space, resulting in a rapid drop in temperature.

6. Numerical simulation

In order to verify whether the observation results described above are correct, and to understand the features of thermal snap on the solar array paddle, we conducted numerical simulation of the solar array paddle. There are many studies analyzing the thermal snap (Thornton, 1996; Boley, 1972; Johnston, 1998; Lin, 2004; Xue2007), we develop the method using a thermal model and a structural model and revising these models by applying the observed data. This section presents the analytical system that we constructed, the result of a thermal-structural analysis and its problems. To solve the problems, we have developed a new model in considering the effects of hinge/latch mechanisms and friction. The result of using new model is also introduced.

## 6.1. Thermal snap analysis procedure

This section describes the thermal snap analysis procedure. Fig. 12 shows a flowchart of thermal snap analysis. The analysis can be broken down into to three parts: construction of the structural model, calculation of temperature distribution, and thermal snap analysis for the penumbra.

In the first part, a structural model of the solar array paddle is constructed for thermal snap analysis. To verify the structural model, we conducted modal analysis to obtain the natural frequency and vibrational mode of the solar array paddle model. These results will be compared with an on-orbit preliminary experiment, and if necessary, we will then revise the model (see Section 6.2 for details). In the second part, a thermal model is developed for the solar array paddle. Thermal analysis for the whole orbit is then conducted to verify the thermal model. The thermal analysis results will be applied to GOSAT's trajectory information, and also compared with data obtained by GOSAT, in order to verify accuracy. After accuracy is verified, thermal analysis will focus on GOSAT during its integration and testing. In order to improve the accuracy of thermal analysis, a profile of thermal input was determined based on the brightness of the solar paddles (see Section 6.3 for details).
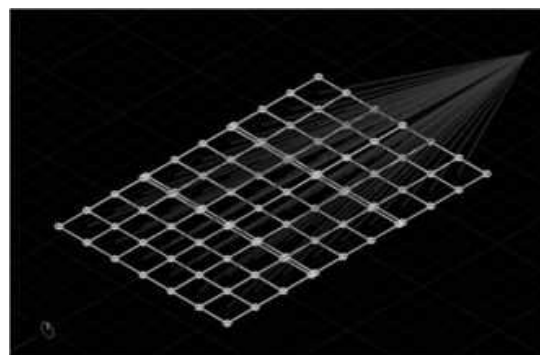
In the third part, the thermal snap analysis is conducted using the structural FEM model of GOSAT.

Fig. 10 and Fig. 11 below show the structural model and the thermal model, respectively.
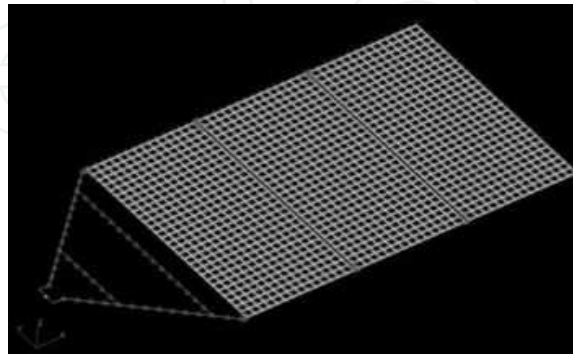

Figure 10. Structural model

Figure 11. Thermal model

## 6.2. Improvement of the structural model

In constructing the structural model of GOSAT's two solar cell paddles, we were not al‐ lowed to access the detailed satellite design data. Therefore, the structural model was based on partly assumed data. Moreover, it is difficult to estimate the production errors on GO‐ SAT. We thus compared the structural model design data and the observation data. The pre‐ liminary observation of solar cell paddle motion was made as GOSAT conducted orbit‐ raising maneuvers using the 20 Newton Gas Jet thrusters. This maneuvering applied relatively large force to the satellite's main body, thereby causing large bending of the solar

cell paddles, followed by the induced vibration thereof. An earlier paper in this series re‐
ported the measurement results.
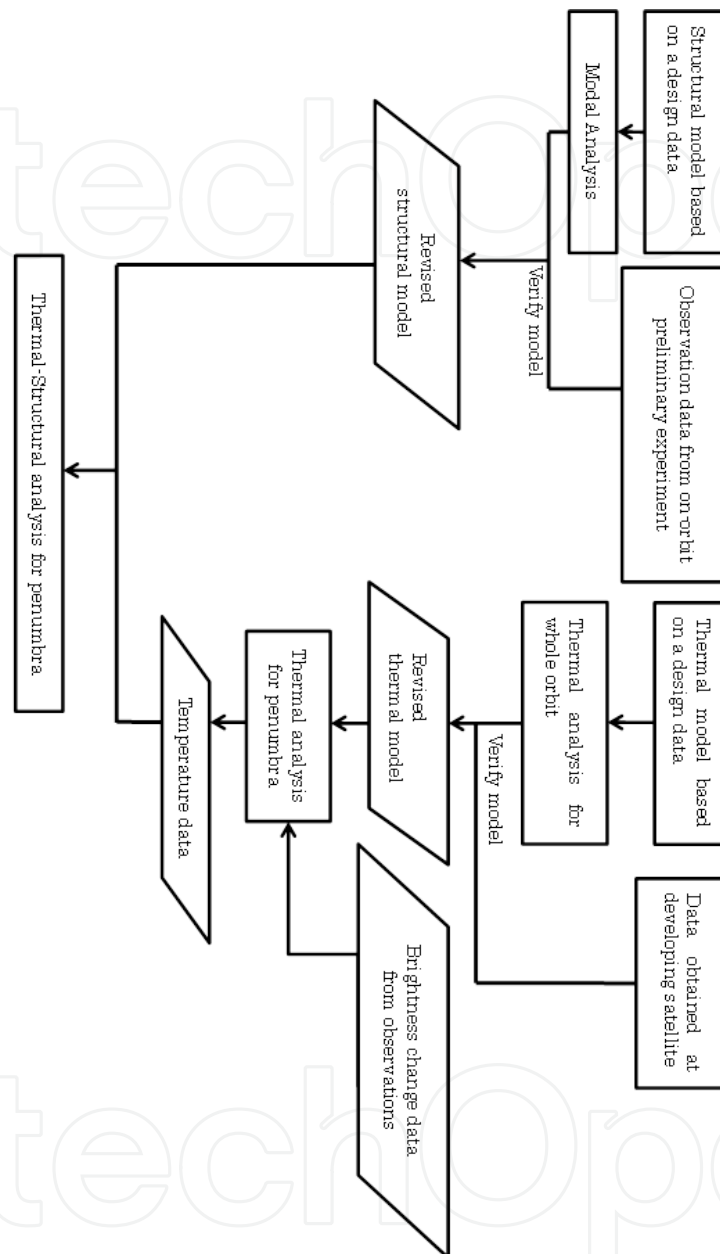
Figure 12. Flowchart of thermal snap analysis using observed data

In this experiment, we severely shook the solar paddle with the 20N thrusters, in order to observe its behavior. The FFT data obtained from this experiment on solar paddle vibration is available. Fig. 13 shows an example of the obtained FFT data. From these data, the natural frequencies of the actual solar array paddle were assumed to be 0.215 [Hz] (out-of-plane) and 0.459 [Hz] (in-plane). These natural frequencies are identical to those obtained by analy‐ sis during development.
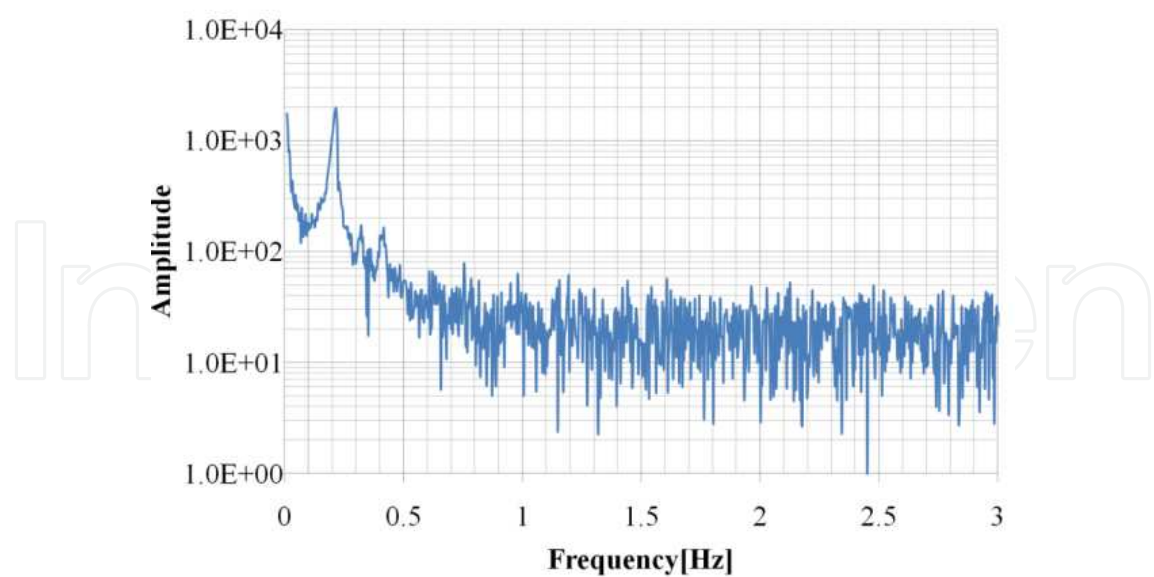
Figure 13. Example of FFT data on out-of-plane solar array paddle vibration as obtained from observation

Next, we conducted modal analysis of the structural model of the solar array paddle to calculate the natural frequency. In case of any differences between the analysis results and observation results, we adjusted the structural data around the root of the solar cell paddles.

By iterating this process, the structural model was revised to generate data similar to that obtained from the solar array paddle in orbit.

Tab. 1 below lists shows the final modal analysis results of natural frequency; Fig. 14 shows the modal shapes of the structural model. From these data, the modal analysis results of the revised structural model match the observed data. Hence, we expect that the revised model could sufficiently simulate the actual solar array paddle.

| Mode number	Frequency [Hz]	Modal shapes
1	0.218	First order out-of-plane
2	0.454	First order in-plane
3	1.262	First order twist
…	…	…

Table 1. Modal analysis results

6.3. Detailed thermal input profile from observed data

During the time when passing the boundary between the sunlight area and umbra area, the thermal environment changes gradually. To conduct thermal snap simulation, a detailed

thermal input profile is needed, but estimating changes from trajectory information alone is difficult due to atmospheric effects. We thus estimated the value of solar light incident (i.e. dominant factor in thermal input) from the brightness value of images taken in observation. By using gray-scale processed images, we assume that if the average gray scale value of an image is max, then the value of solar light incident will also be max. If it is minimum, then the value will be minimum. Fig. 15 shows the estimated solar light incident and total thermal input profile. From the result, we can see that GOSAT's actual optical environment changes gently three times, as long as the value is forecast based on geometric calculation of the satellite's trajectory.
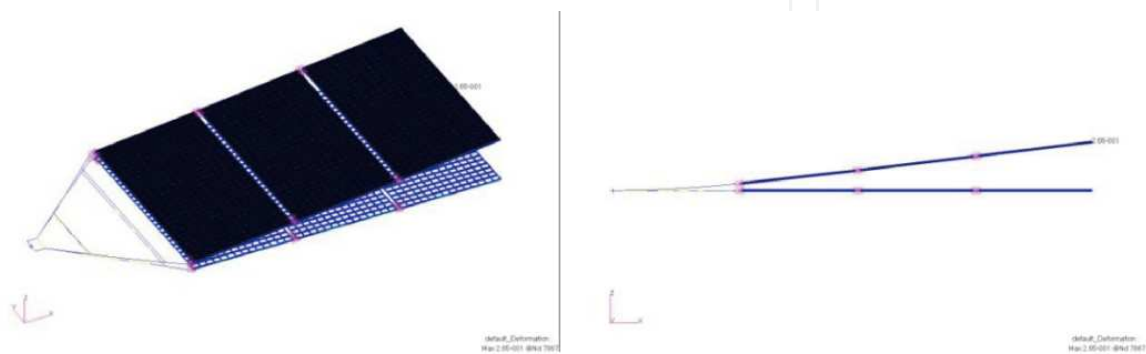
Modal shape for first order, out-of-plane vibration
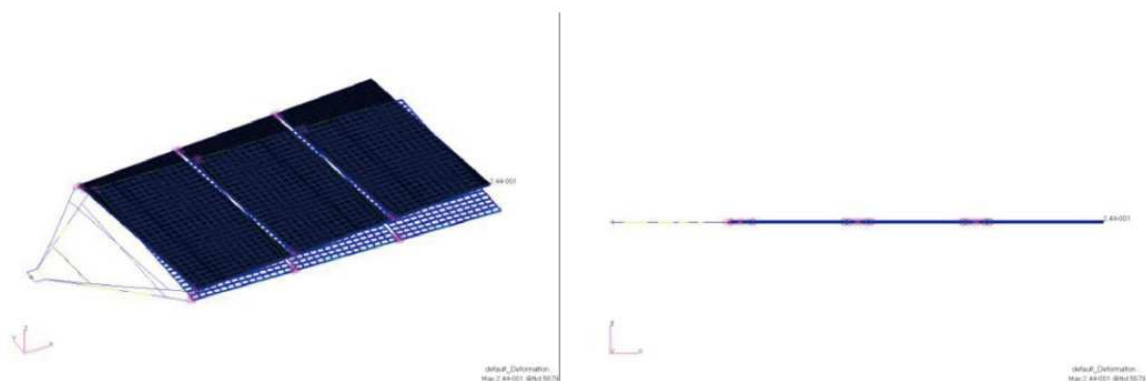
Modal shape for first order, in-plane vibration

Figure 14. Modal shapes of the structural model (Out of Plane and In-Plane Vibration)

By using the thermal input profile thus revealed, we conducted thermal analysis for the penumbra. Fig. 16 shows the simulation results of solar paddle temperature and the values of thermometers. The thermometers are attached at two points. However, no temperature sensor was attached on the front (solar cell; optical incidence) side of the solar paddle, but one was attached only on a backside plane (radiation plane; indicated as Bottom CFRP in Fig. 16). The tendency of simulated solar paddle temperature is similar, however, to the actual data. We therefore conclude that our thermal analysis can sufficiently simulate actual thermal changes.
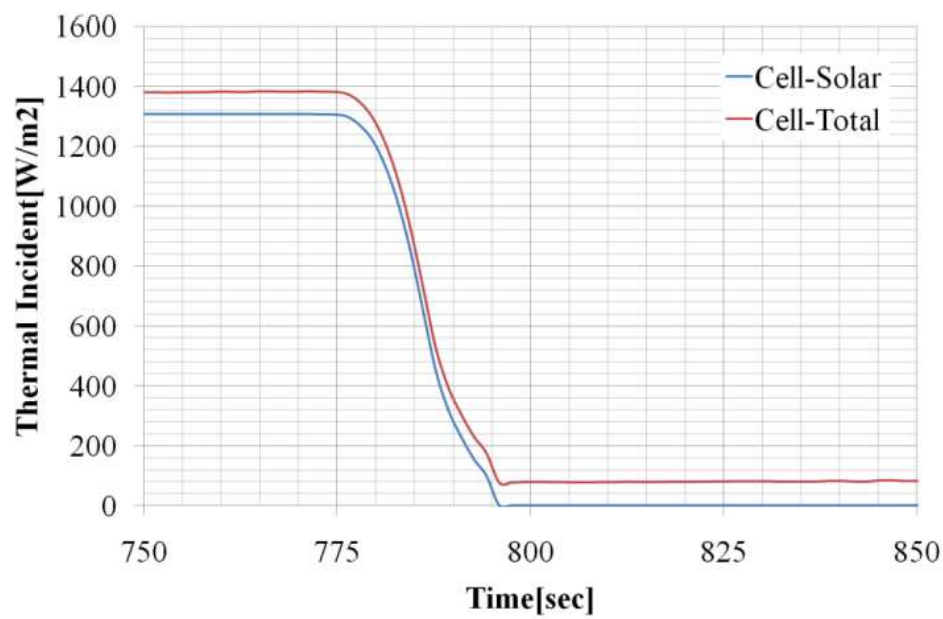
Figure 15. Estimated solar light incident and total thermal input profile from images
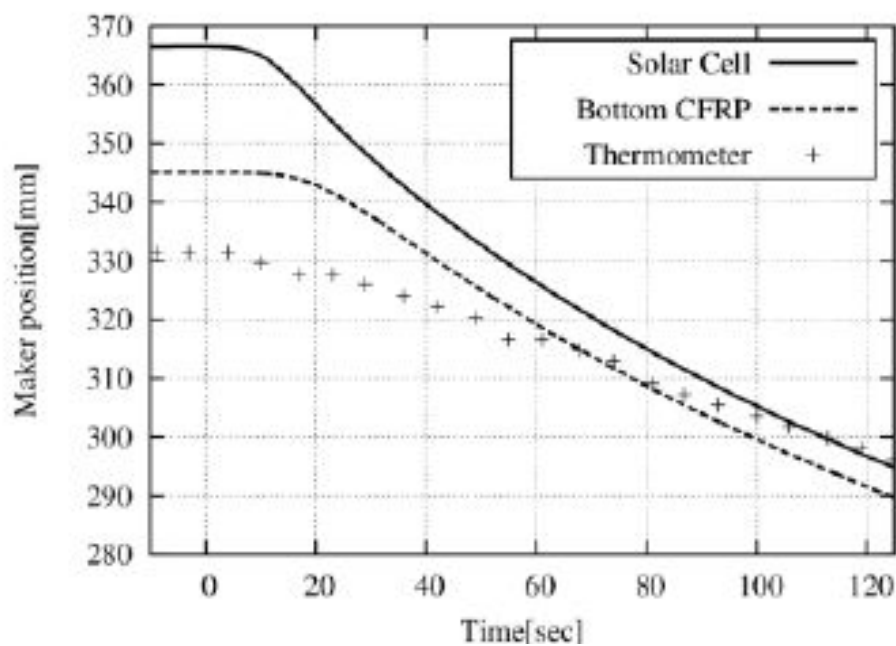
Figure 16. Estimated solar array paddle temperature and values of thermometers attached on a backside plane (Bottom CFRP)

6.4. Results of thermal snap analysis

Thermal snap analysis is conducted using the revised structural model and temperature distribution. Fig. 17 shows the results of thermal snap analysis in the penumbra. The simula-

tion data shows that the solar array paddles will bend in quasi-static while the paddle is illuminated by the Sun. And from the deformation plot, it is assumed that the wires have a large effect on a deformation.

By using the models, we conducted thermal deformation analysis for the whole orbit—a task not possible through camera observation alone. Fig. 18 shows the results. It shows that much larger deformation occurred in the penumbra than at any other time.
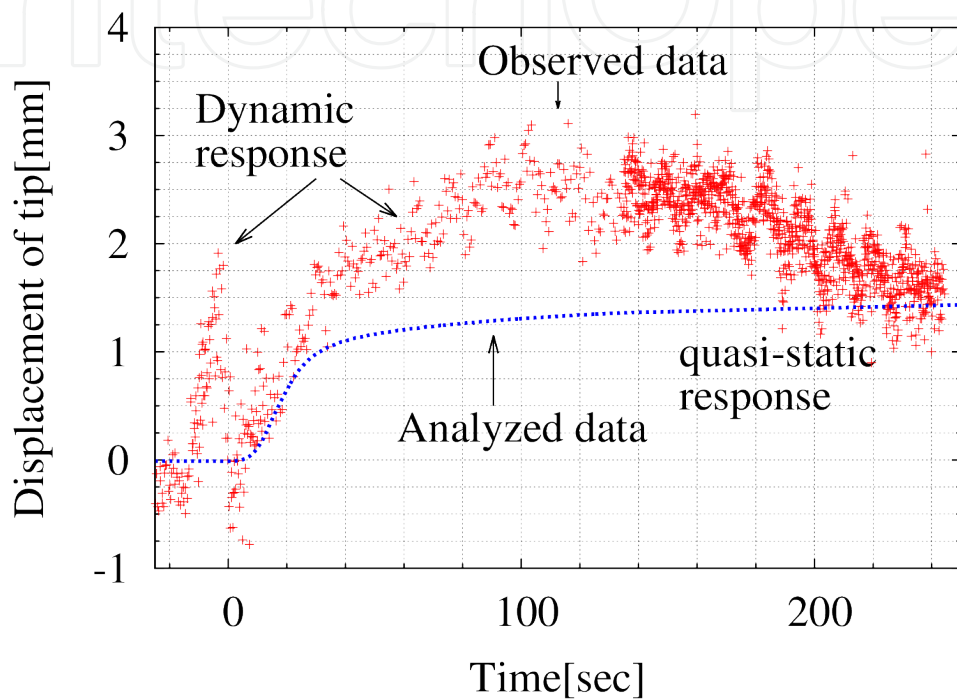
Figure 17. Analysis results of deformation in penumbra
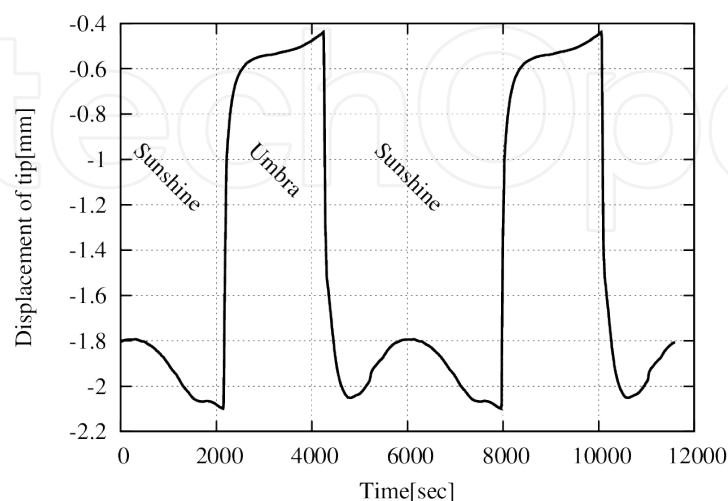
Figure 18. Solar array paddle deformation for two round orbit (The orbital period of GOSAT is 6000 [sec].)

6.5. Detailed modeling for hinges

As dynamic response offers the possibility of adding more awkward disturbances to atti-
tude stability than quasi-static deformation, we decided to check the penumbra data in de-
tail. The observed data obtained in the penumbra indicates that the solar array paddles have
a much lower natural frequency. Fig. 19 shows the FFT data on out-of-plane deformation in
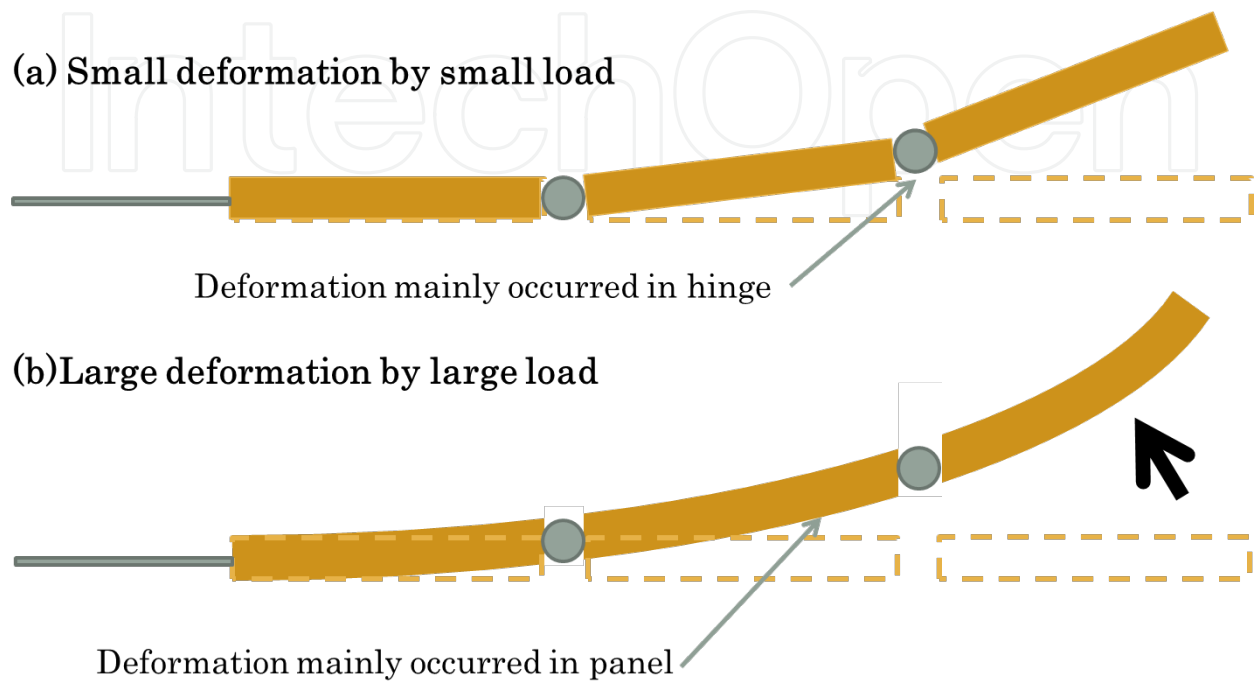the penumbra.
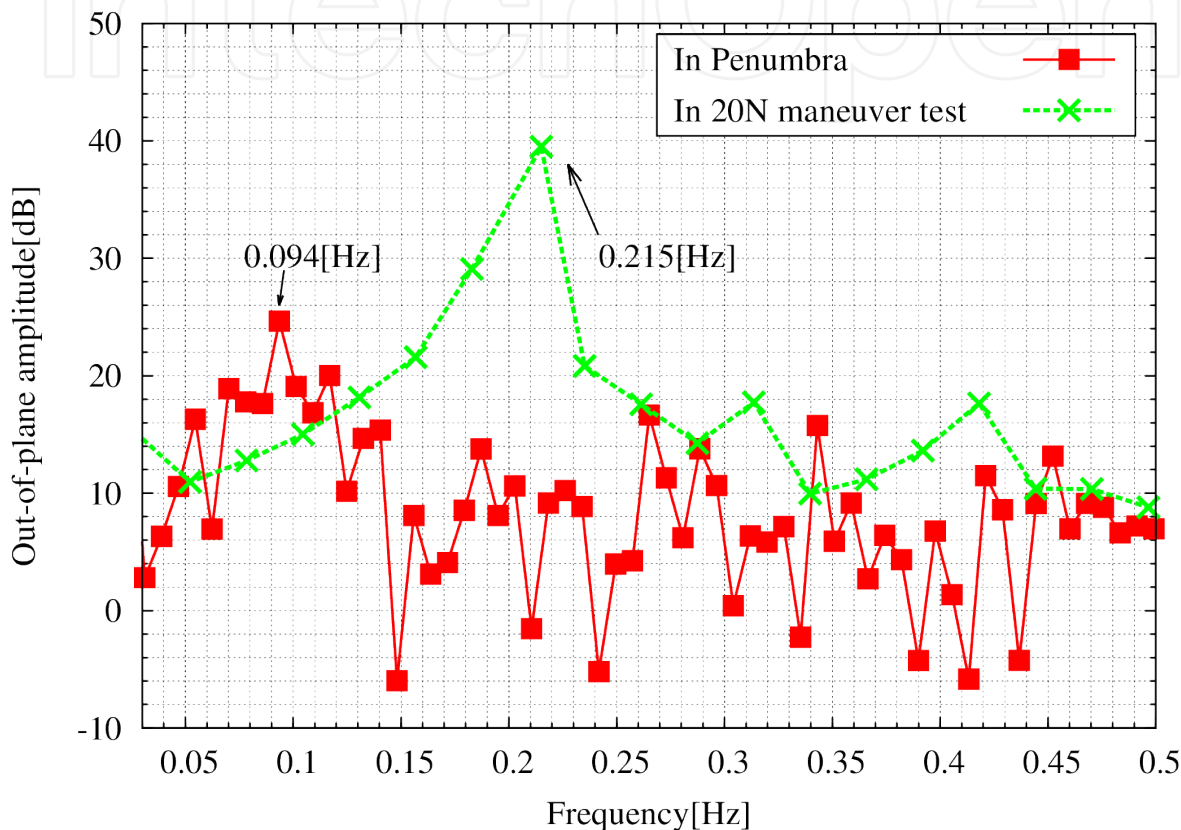
Figure 19. FFT analysis of out-of-plane deformation in the penumbra and same data obtained when maneuvering to
raise orbital altitude using powerful 20N thrusters

Fig. 19 shows the data obtained when using the powerful 20N thrusters to raise GOSAT's
orbital altitude, with vibration of 0.215 [Hz] being observed. When the satellite goes into
eclipse, however, the data obtained did not reveal vibration of 0.215 [Hz], but instead
showed a lower frequency of 0.094 [Hz]. Similar data was not reported during the satellite
integration and qualification tests.

From these reasons, we assumed that the small load (e.g. solar pressure) acts on the solar
panels, and that this load acts as rotation torque at each hinge. As all solar cell panels of GO-
SAT are linked together to maintain the angle of deployment to the deployed position, the
small motion generated at each hinge will also act on all the hinges.

Vibration will occur at each hinge that connects each solar cell panel. Hinges and wires are
used to interconnect the solar cell panels, in order to deploy the solar cell panels and main-

tain the open position of each panel. As each hinge will have some backlash and in order to pull each panel to the deployed position, wires are used to maintain the deployed position after each panel is deployed, and to connect the solar panels, resulting in only a small load under microgravity conditions. Fig. 20 and 21 shows the concept.

(a) Small deformation by small load

Deformation mainly occurred in hinge

(b) Large deformation by large load

Deformation mainly occurred in panel

Figure 20. Concept of vibration affected by the hinge gap
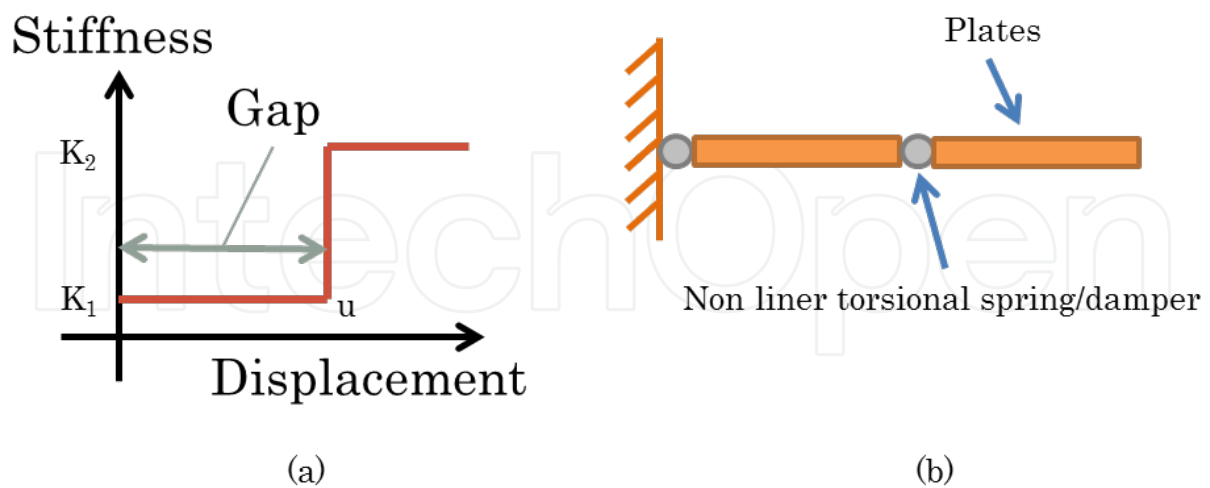
Figure 21. Concept of a hinge modeled using a nonlinear torsional spring. In Fig. 21, (a) shows how to define the stiffness of torsional springs; (b) shows the model for the solar paddle.

Should a small load (e.g. thermal stress) be applied to the solar paddle, deformation will mainly occur in the hinges that have small gaps. Conversely, in case a large load (e.g. inertia

force at maneuver) is applied, deformation of the solar paddle is typically larger than the gaps; therefore, such deformation is mainly caused by the elastic deformation of the panels.

To simulate the effect caused by hinges with a gap, we modeled the hinges with nonlinear torsional springs. In Fig. 21, (a) shows how we added nonlinear characteristics to the torsional springs. The length of u is used to define the gap size. And stiffness within the gap is defined by K_1. When the whole dynamic response shown in Fig. 17 is assumed to have occurred within gap area, the gap width is easily defined. Then, the stiffness of the gap is defined as shown below.

To estimate stiffness, the modeling method for the model of spring-connected plates is used (Kojima et al., 2004). The rotational motion equation for the model of spring-connected plates as shown in Fig. 21 (b) is:

$$I\theta + K\theta = 0 \tag{1}$$

where, I denotes the inertia moment of plates and K the stiffness of torsional springs. Here, given harmonic vibration in which frequency is , the stiffness of gap area K is expressed as:

$$K = I\omega^2 \tag{2}$$

1 is 0.094 [Hz]. Therefore, we assumed the stiffness of gap area K as about 1.21 [Nm/rad] at first, and adjust the value until the vibration properties in penumbra coincide with the value of the observation results.

By using the new model with a detailed hinge, we conducted frequency response analysis. The analysis targets were both a small load condition and a large load condition shown as Tab.2. Fig. 22 shows the results. From the results, we can see that the new model could simulate the vibration occurring in the 20N maneuver test and in the penumbra at the same time.

Excitation force	Condition 1	0.4 [m/s²] inertia force
	Condition 2	7.2 [µPa] pressure on top side
Solver		General-purpose non-liner analysis software "MSC. Marc 2011"
Frequency interval		0.1[Hz]
BC		Tip of york : Fixed
Number of nodes		7903
Number of elements		8292

**Table 2.** Details of frequency response analysis
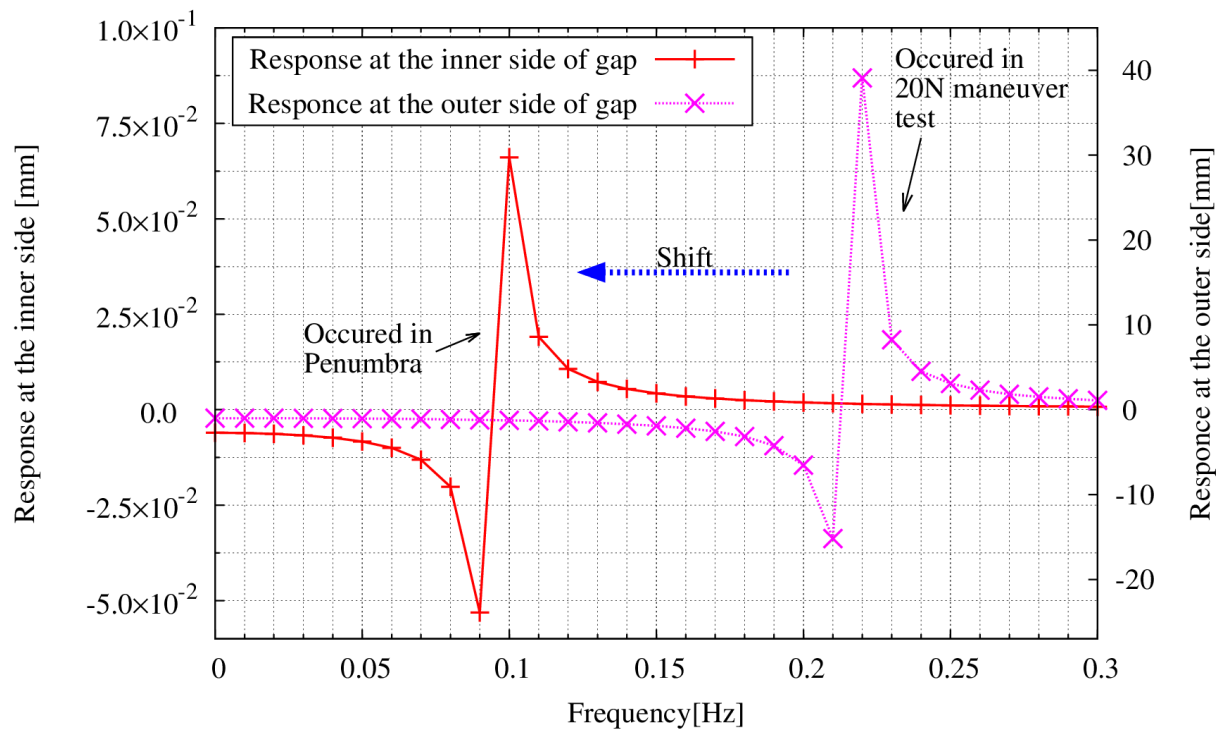
Figure 22. Frequency response analysis results of a structural model with a hinge gap. The analysis of response at the inner side of the gap simulates the dynamic regime in the penumbra. The analysis of response at the outer side of the gap simulates the dynamic regime in the preliminary experiment using the 20N thrusters of GOSAT (see Section 6.2). From the results, the new model with a nonlinear hinge demonstrated that it could simulate the peak shift in response showed in the penumbra (Fig. 19).

# 7. Modeling of stick-slip motion between wires and pulleys

The conventional simulator also had a problem about amplitude of the dynamic responses shown as Fig.17. The slowness of the temperature change in the paddle might be the reason for that. As shown in Fig.16, the significant decreasing of temperature began 5-10 seconds after going into penumbra. While discussing about the dynamic responses, we take notice of some particular measured data (showed in Fig.23). In the data, the solar array paddle shows the characteristic triangular wave before eclipse and the smaller dynamic responses than ordinary one. These triangular waves are found commonly in cantilever vibration affected "Stick-Slip phenomenon" (Maekawa, et.al., 2008). The Stick-Slip is a phenomenon that it arise the "stick" and "slip" behavior continuously to objects shared sliding surfaces. The phenomenon arise on the ground that the change of friction coefficient. And in slip phase, the stored strain energy is released at once. The Stick-Slip phenomenon occurred at space systems had precedents in Hubble Space Telescope (Thomton, 1993). Then, we assumed that the Stick-Slip phenomenon was occurred at deploy-speed-control wires and pulleys. That is because that the wires have small heat capacity and will be great affected by thermal environment changes. And the wires were empirically-deduced that govern the deformation of solar array paddle. The picture of them is shown in Fig. 24, and the position relation is indicated in Fig. 25. When

simulating the thermal snap, sometime these specific dynamic conditions are needed to be considered. For example, when the analysis for Hubble Space Telescope was conducted, the effect from specific cross-section shape of boom was estimated. (Foster, 1995) In case of ADEOS, the tension control mechanism was evaluated in detail. (Taniwaki, 2007)
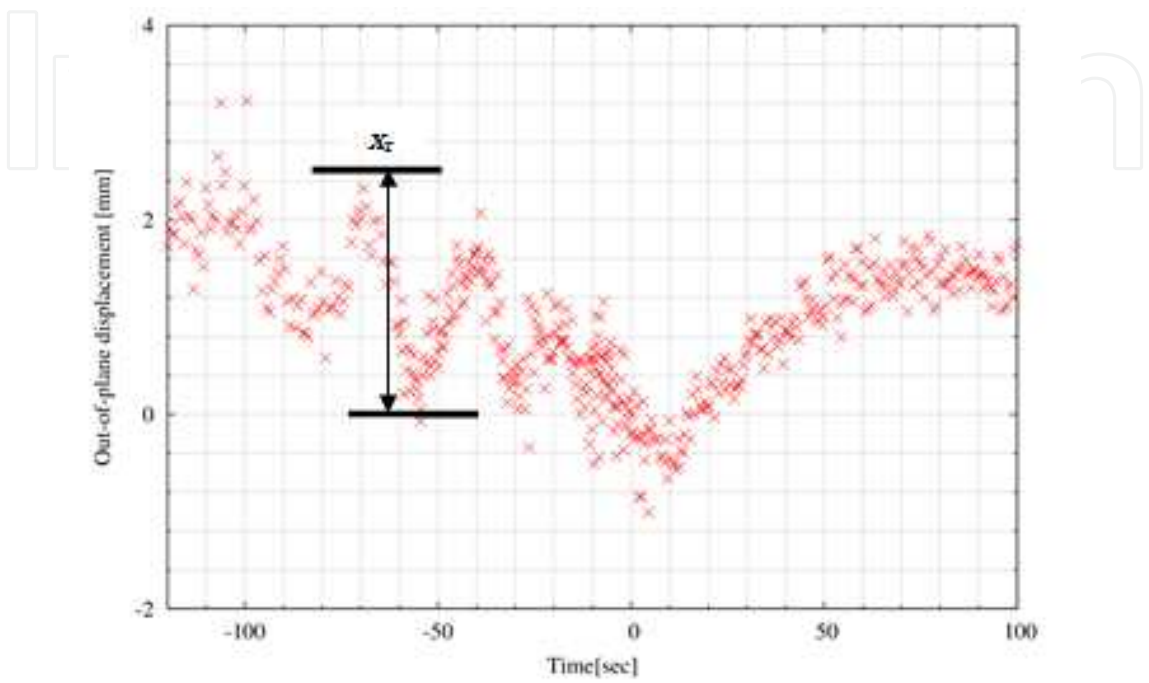
Figure 23. Particular example that solar array paddle shows unexpected behavior.
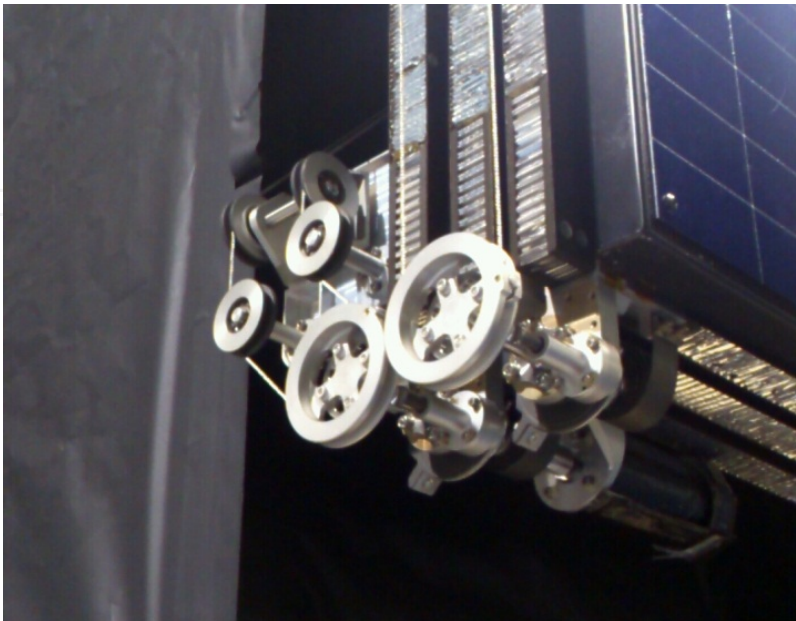
Figure 24. Similar product of GOSAT's Deploy-speed-control wires and pulleys.
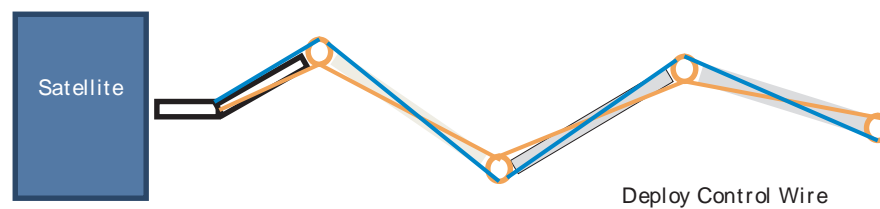
Figure 25. Position relation of GOSAT's Deploy-speed-control wires and pulleys.

To verify the effect of Stick-Slip phenomenon, the phenomenon was introduced to the structural model. In that time, the detailed information of wires and pulleys were not available. Therefore the value from measured data was used to demonstrate the effect of Stick-Slip phenomenon. Using the Bowden and Leben's equation (Bowden & Leben, 1939), the force change while the transition to the slip phase was estimated like below.

$$F_d = x_r k \tag{3}$$

Where the x_r is a displacement defined like showed in Fig.23, and the k is a stiffness of the deformation.
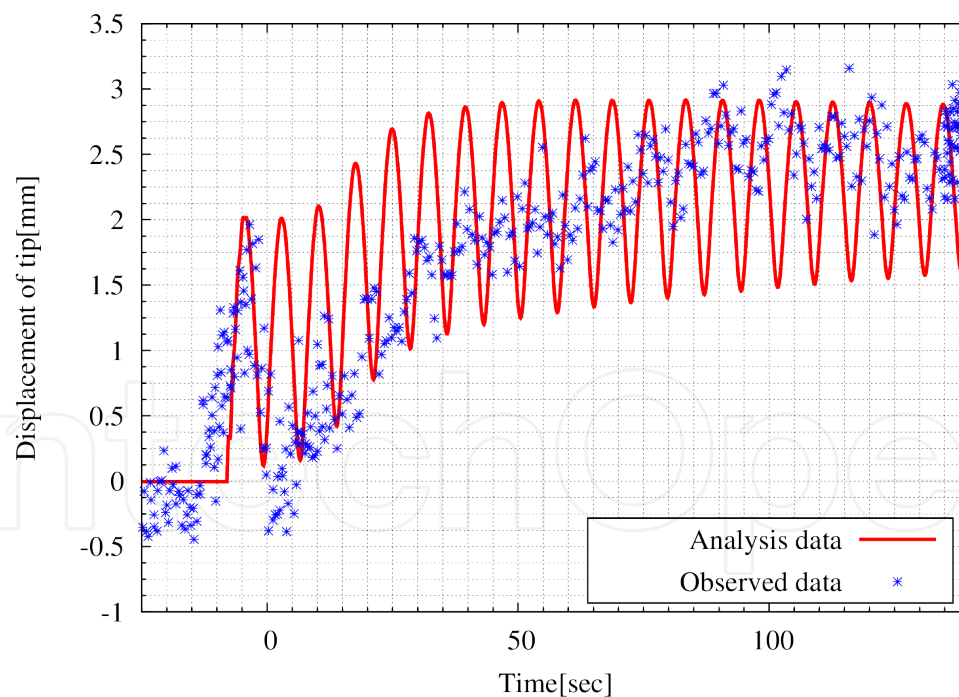
Figure 26. Time transient response simulation with detailed hinge model and stick-slip motion modeling.

From the Fig. 23, the released force was estimated like $F_d \fallingdotseq 0.029$[N]. Using this value, the new simulator was constructed, and verification analysis was conducted. In this analysis, the damping element of paddles was not concerned. The details of analysis are showed in

Tab.3. And the result of analysis is in Fig.26. As shown in Fig.26., the revised simulator could indicate roughly same value of amplitude of dynamic responses with consideration of Stick-Slip phenomenon

Analysis type	Thermal-Structure Time transient
Solver	MSC.Marc 2011
Time step	0.1[sec]
Analysis time	360[sec] (After 770[sec] of static state analysis)
BC	Tip of york : Fixed
	Temperatures of Top panel, Bottom panel, wires. Given by thermal model

Table 3. Details of thermal snap analysis

8. Conclusions

When a satellite in Low Earth Orbit (LEO) goes through an eclipse, sudden changes in the thermal environment will occur. These sudden thermal changes caused by a difference in temperature between the Sun side and the opposite side of the satellite's solar array paddle. This temperature difference causes bending and then vibration of the solar array paddle. However, the bending and vibration amplitude are too small to be observed by conventional satellite attitude sensors. To solve this problem, we used an onboard camera to directly measure solar paddle bending. The previously reported methods of observing the motion of the satellite's solar array paddle were not free from errors in image data processing, especially when the object was weakly illuminated by the Sun.

This chapter paper described the improved image data processing algorism applied to measure bending and deformation of the satellite's solar array paddle that are believed to cause degraded satellite attitude stability, which occurs when the satellite goes into an eclipse. The revised observation data shows both quasi-static deformation and rapid dynamic vibration in the penumbra. We also conducted numerical analysis to verify the observed data and understand the features of thermal snap on the solar array paddle. From this analysis, we found that sudden changes in solar array paddle temperature induce quasi-static deformation, and that the wires controlling solar array paddle deployment have a large influence on solar array paddle vibration. Additionally, we also found that a specific lower frequency vibration appearing in the penumbra can help to explain this vibration mechanism. Developing the detailed hinge model, we succeeded to simulate the vibration property change related to dynamical regime. Then, we focused on the specific results of observation and assumed that Stick-Slip phenomenon have a great influence on behavior of paddles. To simulate the influence, we revised the structural model and conducted the ther-

mal snap analysis. The result indicated the gap of hinges and Stick-Slip phenomenon mainly effect on dynamical response of thermal snap on GOSAT.

As ongoing work, we will model the Stick-Slip phenomenon more in detail and introduce the damping element using observed data.

Author details

Mitsushige Oda[1], Akihiko Honda[2], Satoshi Suzuki[3] and Yusuke Hagiwara[4]

1 JAXA and Tokyo Institute of Technologies, Japan

2 Tokyo Institute of technology, Japan

3 Advanced Engineering Services Co.Lted, Japan

4[4]Mitsubishi Heavy Industries, Ltd, Japan

References

[1] B., A. Boley(1972), Approximate Analyses of Thermal Induced Vibrations of Beam and Plates, *Journal of Applied Mechanics*, vol. 39, no. 1, pp212-216

[2] Chijie Lin, Ramesh B. Malla(2004), Coupled Thermo-Structural Analysis of an Earth Orbiting Flexible Structure, in 45th AIAA/ASME/ASCE/AHS/ASC Structures, Structural Dynamics & Materials Conference, AIAA2004-1793

[3] Earl, A. Thomton, Yool A. Kim(1993): Thermally Induced Bending Vibrations of a Flexible Rolled-Up Solar Array, Journal of Spacecraft and Rockets, Vol.30, No.4, pp438-448

[4] E., A. Thornton (1996), Thermal Structures for Aerospace Application, AIAA, pp. 343-354

[5] F. P. Bowden & L. Leben (1939): The Nature of Sliding and the Analysis of Friction, *Proceedings of Royal Society London,* vol.A169, pp371-391

[6] Foster, C. L., Tinker, G. S., Nurre, W. & Till, W. A. (1995). NASA Technical Paper, The Solar

[7] Array-Induced Disturbance of the Hubble Space Telescope Pointing System, 3556

[8] Japan Society of Mechanical Engineering (February 2007). Mechanical Engineers' Handbook Applications 11: Space Equipment and Systems, Japan Society of Mechanical Engineering, ISBN 978-4-88898-154-5, Japan

[9] John D.Johnston, Earl A. Thornton(1998), Thermally Induced Attitude Dynamics of a Spacecraft with a Flexible Appendage, *Journal of Guidance, Control, and Dynamics*, vol. 21, no. 4, pp. 581-587

[10] Kojima, Y., Taniwaki, S., & Ohkami, Y. (2004): Attitude Vibration Caused by a Stick-Slip Motion for Flexible Solar Array of Advanced Earth Observation Satellite. *Journal of Vibration and Control*, Vol. 10, No. 10, 2004, pp.1459-1472.

[11] Ming-De Xue, Jin Duan, Zhi-Hai Xiang(2007), Thermally-Induced bending-torsion coupling vibration of large space structures, Comput Mech, vol. 40, pp.707-723

[12] Mobara, M. (1994). Introduction to aerospace engineering guidance and control of satellite and rocket, Baifukan, ISBN 978-4-56303-493-1, Japan

[13] Oda, M., Hagiwara, Y., Suzuki, S., Nakamura, T., Inaba, N., Sawada, H., Yoshii, M., & Goto, N. (2011): Measurement of Satellite Solar Array Panel Vibrations Caused by Thermal Snap and Gas Jet Thruster Firing. *Recent Advances in Vibrations Analysis*, In-Tech, ISBN 978-953-307-696-6, Croatia.

[14] S, Maekawa, K, Nakano (2008): Relationship between Schallamach waves in contact surfaces and stick-slip in sliding systems, Manuscript of JAST Tribology Conference 2008, pp81-82

[15] Taniwaki, S., Kojima, Y., Ohkami, Y. (2007), Attitude Stability Analysis for Stick-Slip-Induced Disturbances of Extended Structure with Tension Control Mechanism, Journal of System Design and Dynamics, vol. 1, No. 4, pp714-723